

# MULTIPLE-DEMAND SYSTEM IDENTIFICATION AND CHARACTERIZATION VIA SPARSE REPRESENTATIONS OF fMRI DATA

Xiang Li<sup>1</sup>, Qinglin Dong<sup>1</sup>, Xi Jiang<sup>1</sup>, Jinglei Lv<sup>1</sup>, Tianming Liu<sup>1</sup>

<sup>1</sup>Cortical Architecture Imaging and Discovery Lab, Department of Computer Science and Bioimaging Research Center, the University of Georgia, Athens, GA.

## ABSTRACT

Identification of concurrent spatially overlapping functional networks and understanding of their mechanisms of jointly realizing the total brain function have been important yet challenging problems. In this work, we have applied a data-driven sparse representation framework to learn a dictionary consisting of multiple network components and their associated weight coefficients from a given fMRI dataset. Then we analyzed the network component composition at the voxel level by correlating component weights to the characteristics of regions with strong involvements in multiple components, which are defined as functionally highly heterogeneous regions (HHR). Consequently, the spatial overlap of HHRs obtained across multiple tasks of a given subject is defined as the multiple-demand (MD) system. By applying the proposed framework on the recently publicly released Human Connectome Project (HCP) task fMRI dataset, we have obtained reproducible HHR and MD systems that concentrated on the frontal and parietal cortex. Interestingly, the spatial distribution of those MD regions has been found to be highly correlated with the cortical folding and structural connectivities, revealing closely related brain structural and functional architectures.

**Index Terms**—Functional network, dictionary learning, multiple-demand system, structural-functional relationship

## 1. INTRODUCTION

In the field of functional neuroimaging analysis, there has been increasing literatures investigating the spatial and temporal characteristics of functional networks in brain. It has been well recognized that brain function is mediated by functionally distinct yet spatially overlapping networks [1] and the brain’s functional integration will require “large scale neuronal dynamics sharing a substantial anatomical infrastructure” [2]. Recently, multiple-demand (MD) system with general-purpose machinery and highly heterogeneous functional profiles has been located at the frontal and parietal cortex using various methodologies [3, 4].

However, the fact that certain brain regions can be part of multiple functional networks makes them difficult to be identified by traditional analysis approach (i.e. activation detection by the general linear model (GLM)) [5, 6]. In this work, we propose a sparse representation framework to

identify the MD system in task fMRI (tfMRI) data. In the first step, tfMRI signals over the whole-brain of an individual are decomposed into hundreds of over-complete dictionary components using dictionary learning method along with the weight vectors that are the corresponding regression coefficients [9-10]. In the second step, the weight vectors obtained by the dictionary learning on each tfMRI dataset of each subject are examined to investigate the component composition of each region in the brain. Regions with multiple high values in their weight vectors, indicating high involvement in multiple functional network components, are defined as highly heterogeneous regions (HHR) of that task. Then the multiple demand (MD) system is defined by the consistently occurring HHRs over multiple tasks of the same subject.

The proposed framework has been applied on the dataset provided by the recently publicly released Human Connectome Project (HCP) Q1 dataset [7]. The results revealed two important characteristics of the identified MD system: 1) MD systems identified over multiple subjects show a similar spatial pattern that mainly concentrates on the parietal cortex as well as scattered around the frontal cortex; 2) Interestingly, by analyzing the cortical folding patterns and DTI-derived fiber density on the MD system, we have found that there exists a strong and groupwise consistent relationship between the data-driven functionally-derived MD system with the cortical folding patterns and the structural connectivity profile.

## 2. MATERIALS AND METHODS

### 2.1. Data acquisition and pre-processing

We have applied the proposed model on the Human Connectome Project tfMRI dataset consisting of 68 subjects scanned in 7 tasks. The scan length varies between tasks from 2 to 5 minutes (176 volumes to 405 volumes). The acquisition parameters are: 90×104 matrix, 220mm FOV, 72 slices, TR=0.72s, TE=33.1ms, flip angle = 52°, BW =2290 Hz/Px, in-plane FOV = 208 × 180 mm, 2.0 mm isotropic voxels. The preprocessing pipeline includes motion correction and slice time correction. The signals were then normalized to zero mean and unit standard deviation. More details of the experiment design, behavior measurements and activation maps can be found at [7]. Then linear registration using FSL FLIRT was performed on the fMRI dataset to DTI space for the later cortical surface wrapping.

## 2.2. Dictionary learning on fMRI data

The pre-processed brain functional fMRI signals  $S$ , which is a  $(T \times N)$  matrix consisting of  $T$  volumes and  $N$  voxels for each task each subject are then used as the input for the  $l_1$  norm regularized dictionary learning scheme. Using a publicly available online dictionary learning method SPAMS [9], the fMRI signals on  $N$  voxels are modeled as the linear combinations of the learned dictionary  $D$  with weight matrix  $\alpha$  by solving the optimization problem:

$$\min_{D \in \mathbb{R}^{T \times K}, \alpha \in \mathbb{R}^{K \times N}} \frac{1}{2} \|S - D\alpha\|_2^2 + \lambda \|\alpha\|_1 \quad s.t. \forall j = 1, \dots, K, D_j^T D_j \leq 1$$

where the constraint on the learned dictionary  $D_j^T D_j \leq 1$  refrains the optimization from getting the trivial solution.  $D$  and  $\alpha$  will be alternatively solved based on gradient descent algorithm in the optimization procedure, and the optimization is converged when the change of overall error is smaller than a given value  $\epsilon$  (set as 1% in this work). The learned dictionary  $D$  consists of  $K$  ( $T < K \ll N$ ) number of components, each is a time series with the same length  $T$  serving as the basis for sparsely regressing the input whole-brain fMRI signals. Correspondingly, fMRI signal on the  $i$ -th voxel is regressed by those  $K$  basis with the corresponding weight vector  $\alpha_i$ . In this work, the component number  $K$  and the regularization parameter  $\lambda$  were all determined experimentally ( $K=400$ ,  $\lambda=0.01$ ) [9-10]. It has been tested that within a reasonable range, the parameters will not affect the model performance much.

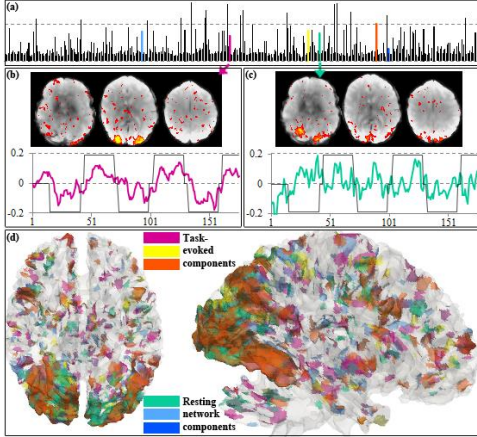


Fig.1. Illustration of the dictionary learning/sparse representation framework and the spatial overlaps across network components. (a) Summed absolute weight value of the  $K$  components learned from the emotion task fMRI dataset of a randomly selected subject, indicating their overall area of activation in the brain. Task related and resting-state network components have been highlighted by various colors; (b) Spatial activation map and temporal time series pattern (pink curve) of a specific (187th) component, as well as the paradigm design of the emotion task (black block); (c) Spatial activation map and temporal activation pattern (green curve) of another (264th) component; (d) Three task-evoked components (including the 187th), plus three resting network components (including the 264th), mapped on the cortical surface together. The

cortical surface is color-coded by the color bar on the left, which is correspondent to the colors used in (a).

As an example, a brief illustration of the components obtained by the dictionary learning on emotion data of a randomly selected subject is given in Fig. 1. There are two important facts revealed by their spatial and temporal characteristics: 1) The components, which are obtained from a totally data-driven approach, are neuroscientifically meaningful, as shown in Fig. 1(b) and (c). 2) There is substantial spatial overlap across different components, even between task-evoked and resting network components, which are traditionally regarded as independent from each other. Such observation, especially regarding the component overlap regions in the brain, motivated us to perform more in-depth analysis of the network component composition at voxel level to investigate their detailed characteristics.

## 2.3. Identification of Functionally Highly Heterogeneous Regions (HHR) and the Corresponding Multiple-Demand (MD) System

By examining the voxel-by-voxel weight vectors  $\alpha$  in the learned dictionary results, we have found that there are three types of voxels in the whole brain, considering the fact that the signal of each voxel has been normalized: 1) Voxels with low weights of all basis, indicating that fMRI signals defined on them can not be well-regressed by the dictionary. This might be mainly due to  $l_1$  norm regularization on the cost function which enables larger reconstruction error. 2) Voxels with high weight for a few bases but low weights for other basis. As shown in Section 2.2, some of those voxels can be possibly correlated to task stimulus. 3) Voxels with high weight for multiple components. The collection of such voxels are the main focus of this work, which we called as functionally highly heterogeneous regions (HHR) because of their complex component composition, defined by the following equation:

$$\forall \text{Voxel } i, i \in \text{HHR} \text{ i.f.f. } \sum (\alpha_i | > T_1) > T_2\%$$

Specifically, we count the number of components whose absolute weight value is higher than a given threshold  $T_1$  on each voxel; then we sort all the voxels by the counting value, and take the top  $T_2\%$  of the voxels as HHR. Thus  $T_1$  will affect the composition of the region (larger  $T_1$  will prefer voxels with larger absolute value of  $\alpha$  and vice versa), while  $T_2$  will affect the size of it. It should be noted that the thresholding method is used here because we have observed that the number of components with weight greater than any given threshold over the whole brain is roughly normally distributed, thus the identification of HHR and MD system will not be biased by the threshold value used. An illustrative example of HHR and its relationship with  $T_1$  and  $T_2$  is given in Figs. 2 (a)-2(b).

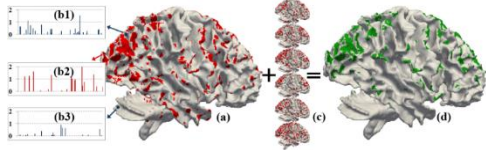


Fig.2. Illustration of the relationships between weight vector, HHR and MD system in the proposed framework. (a) Visualization of HHR of emotion task from a randomly selected subject mapped on cortical surface; (b1) Weight vector  $\alpha_i$  from a voxel (marked by blue dot) with a few high values, thus it will be excluded from HHR but might be included with a lowered  $T_2$ ; (b2) Weight vector from a voxel from HHR with several high values; (b3) Weight vector from a voxel (marked by blue dot) with no high values, thus it will be very unlikely to be part of HHR; (c) HHRs obtained from other 6 tasks from the same subject; (d) MD system obtained from the thresholded summation of the HHRs from 7 tasks ( $\geq 4$ ).

After identifying HHRs for all 7 tasks on a given subject, those HHRs are added together as they are in the same space. Thus we can obtain a new map of the brain on which each voxel is assigned a “multiple-demand” (MD) value ranging from 0 to 7 (as similarly defined in the literature [3, 4]), measuring the frequency the voxel being included in the HHR as shown in Fig. 2. As there are 7 tasks in the HCP fMRI dataset, the collection of voxels with MD values no smaller than 4 (more than half of 7 tasks) is considered as MD system of that subject in this work.

### 3. EXPERIMENTAL RESULTS

#### 3.1. Identified HHR and MD System

As described in section 2.3, given an fMRI dataset consisting of multiple tasks, the HHR and the resultant MD system will be identifiable with thresholding values  $T_1$  and  $T_2$ . By applying our proposed framework on the HCP fMRI dataset using various  $T_1$  and  $T_2$  combinations, we have obtained the dictionary learning results and the corresponding HHR/MD system of 68 subjects with 7 tasks. In this section, we will use the results obtained from the emotion task from a randomly-selected subject as an example to discuss how the parameter setting will affect the results, while the conclusion is similar across all subjects. As shown in Fig. 3, increasing level of  $T_1$  (threshold on weights when counting the components on each voxel) will slightly move the identified HHR from a scattered spatial distribution over the whole brain to the concentration on parietal and frontal cortices, consistent with the spatial distribution of MD system in previous literature reports [3, 4]. On the other hand, the spatial distribution of HHR and MD system from an increased level of  $T_2$  (threshold on the number of voxels included in the HHR) will also be more likely to locate on the parietal cortex.

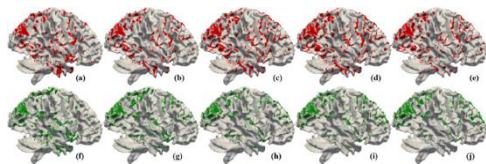


Fig.3. (a)-(e) Visualization of identified HHR of emotion task from the same subject as in Fig. 1 using different  $T_1$  values of 0, 0.1, 0.2, 0.3 and 0.4. (f)-(j) Visualization of MD system of emotion task using different  $T_1$  values of 0, 0.1, 0.2, 0.3 and 0.4. The visualization in Fig. 2(a) and (d) uses  $T_1=0.4$ .

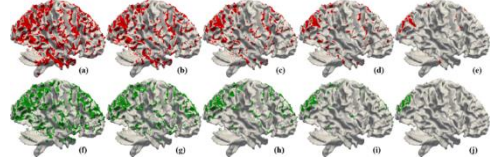


Fig.4. (a)-(e) Visualization of identified HHR of emotion task from the same subject as in Fig. 1 using different  $T_2$  values of 80%, 84%, 88%, 92% and 96%. (f)-(j) Visualization of identified MD system of emotion task using different  $T_2$  values.

#### 3.2. Relationship between MD System, cortical folding pattern and white-matter Fiber Density

The spatial pattern of the MD systems across multiple subjects show an interesting and consistent characteristic, as shown in Figs. 5 (a1), (b1) and (c1), where it is largely located on the gyral regions of the cortical surface. In addition, because of the close relationship between the folding pattern and the structural connectivity profiles of the brain [8], the MD system also tends to have high DTI-derive fiber density, as shown in Figs. 5 (a3), (b3) and (c3), where the fiber density information is obtained using similar method as in [8]. To quantitatively investigate such relationship, we have used the principal curvature (illustrated in Fig. 5 (a2), (b2) and (c2)) as an indicator for the folding pattern, where a positive principal curvature value of a unit region indicates that region is on gyrus and negative value indicates it is on sulcus. Then the numbers of gyrus/sulcus are counted over the unit regions defined by MD system. Finally we used the ratio between gyrus count and sulcus count as a measurement of where the MD system locates. On the other hand, the DTI-derived fiber density provides a natural measurement for characterizing the structural connectivity profile of the MD system, where we averaged the fiber density across each unit region in the MD system, the averaged results over 20 subjects are in table 1.

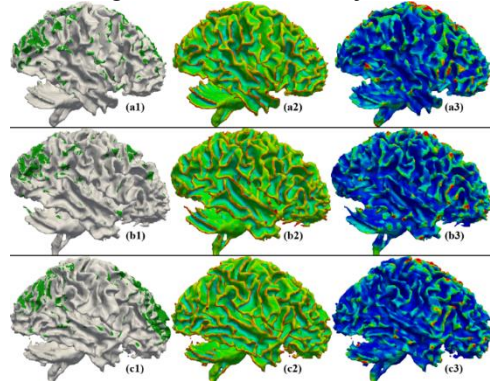


Fig.5. (a1) Visualization of MD system from the same subject as used in Fig. 1; (a2) Same surface color-coded by the principal curvature value; (a3) color-coded by the fiber density; (b1)-(b3), (c1)-(c3) Similar visualizations from other two random subjects;

The groupwise MD system is more likely to be located on the gyrus (all rates greater than 1.3, comparing with whole-brain average rate of 1.13) with higher fiber density (comparing with whole-brain average density=3.95). The trend of the table shows a higher  $T_1$  threshold will result in more gyrus-located MD system, indicating regions that are more intensively involved in multiple networks are more likely to be on gyral area. A higher  $T_2$  threshold will also identify MD system with larger gyrus/sulcus rate, indicating regions that are involved in larger number of networks components are more likely to be on gyrus. Similar trend is also observed in the relationship between MD system and fiber density distribution. In summary, the group-wise consistent result reveals a unanimously close relationship between brain functional integration, cortical folding pattern and structural connectivity. While we have been aware that the effect of different signal-to-noise ratio of the imaging between gyrus and sulcus can be affecting the MD system identification as well as the fiber tracking results, we believe the functional segregation between gyrus/sulcus revealed by the results of this work is neuroscientifically meaningful as supported by previous reports on the concentration of fibers on gyrus in human fetus brains [11], as well as the difference of axonal connectivity and gene expression between cerebellum gyri and sulci in rodent brains [12].

Table 1. Top: Mean fiber density value and its standard deviation of the MD system identified with different thresholding parameter combinations. Bottom: Average gyrus/sulcus rate and its standard deviation of the MD system, arranged in a similar fashion.

Fiber density					
T1\T2	80%	84%	88%	92%	96%
<b>0.000</b>	3.7±0.5	3.8±0.6	4.1±0.8	4.3±1.1	4.7±1.7
<b>0.050</b>	4.0±0.4	4.1±0.5	4.4±0.8	4.7±1.1	4.9±1.6
<b>0.100</b>	4.2±0.5	4.4±0.7	4.6±1.1	4.9±1.4	5.0±1.7
<b>0.150</b>	4.3±0.6	4.5±0.9	4.8±1.2	5.0±1.6	5.1±1.7
<b>0.200</b>	4.4±0.6	4.7±0.9	4.9±1.3	5.2±1.6	5.2±1.8
Gyrus/Sulcus rate					
T1\T2	80%	84%	88%	92%	96%
<b>0.000</b>	1.3±0.1	1.7±0.0	2.0±0.1	2.5±0.2	2.9±0.6
<b>0.050</b>	1.4±0.1	2.0±0.0	2.3±0.1	2.5±0.2	3.0±0.6
<b>0.100</b>	1.5±0.1	2.1±0.1	2.3±0.2	2.5±0.3	3.1±0.5
<b>0.150</b>	1.6±0.1	2.2±0.1	2.5±0.2	2.6±0.3	3.2±0.5
<b>0.200</b>	1.7±0.1	2.3±0.1	2.4±0.2	2.6±0.3	3.1±0.5

#### 4. CONCLUSION

In this work, we have proposed a computational framework for deriving the functionally highly heterogeneous regions and the corresponding multiple-demand system by component compositions. The result by applying the framework on HCP tfMRI datasets showed consistent spatial distribution of the MD system across subjects. The MD system has been found more likely to locate at gyral regions with higher fiber density, revealing close relationships between brain function and structure,

especially the possibility that cortical gyral regions can be the functional hub and multi-functioning center of the brain.

#### 5. REFERENCES

- [1] S. M. Smith, K. L. Miller, S. Moeller, J. Xu, E. J. Auerbach, M. W. Woolrich, C. F. Beckmann, M. Jenkinson, J. Andersson, M. F. Glasser, D. C. Van Essen, D. A. Feinberg, E. S. Yacoub, and K. Ugurbil, "Temporally-independent functional modes of spontaneous brain activity" *Proceedings of the National Academy of Sciences*, 109, (8), pp. 3131-3136, 2012.
- [2] K. J. Friston, "Modes or models: a critique on independent component analysis for fMRI" *Trends in Cognitive Sciences*, 2, (10), pp. 373-375, 1998.
- [3] E. Fedorenko, J. Duncan, and N. Kanwisher, "Broad domain generality in focal regions of frontal and parietal cortex" *Proceedings of the National Academy of Sciences*, 110, (41), pp. 16616-16621, 2013.
- [4] J. Duncan, "The multiple-demand (MD) system of the primate brain: mental programs for intelligent behaviour," *Trends in Cognitive Sciences*, 14, (4), pp. 172-179, 2010.
- [5] N. K. Logothetis, "What we can do and what we cannot do with fMRI," *Nature*, 453, (7197), pp. 869-878, 2008.
- [6] B. Kretzelberg, G. M. Boynton, and R. J. A. van Wezel, "Adaptation: from single cells to BOLD signals," *Trends in Neurosciences*, 29, (5), pp. 250-256, 2006.
- [7] D. M. Barch, G. C. Burgess, M. P. Harms, S. E. Petersen, B. L. Schlaggar, M. Corbetta, M. F. Glasser, S. Curtiss, S. Dixit, C. Feldt, D. Nolan, E. Bryant, T. Hartley, O. Footer, J. M. Bjork, R. Poldrack, S. Smith, H. Johansen-Berg, A. Z. Snyder, and D. C. Van Essen, "Function in the human connectome: Task-fMRI and individual differences in behavior," *NeuroImage*, 80, (0), pp. 169-189, 2013.
- [8] D. Zhu, K. Li, L. Guo, X. Jiang, T. Zhang, D. Zhang, H. Chen, F. Deng, C. Faraco, C. Jin, C.-Y. Wee, Y. Yuan, P. Lv, Y. Yin, X. Hu, L. Duan, X. Hu, J. Han, L. Wang, D. Shen, L. S. Miller, L. Li, and T. Liu, "DICCOL: Dense Individualized and Common Connectivity-Based Cortical Landmarks," *Cerebral Cortex*, 23, (4), pp. 786-800, 2012.
- [9] Lv J., Jiang X., Li X., Zhu D., Chen H., Zhang T., Zhang S., Hu X., Han J., Huang H., Zhang J., Guo L., Liu T., "Sparse Representation of Whole-brain FMRI Signals for Identification of Functional Networks," in press, *Medical Image Analysis*, 2014.
- [10] Lv J., Jiang X., Li X., Zhu D., Zhang S., Zhao S., Chen H., Zhang T., Hu X., Han J., Ye J., Guo L., Liu T., "Holistic Atlases of Functional Networks and Interactions Reveal Reciprocal Organizational Architecture of Cortical Function," in press, *IEEE Transactions on Biomedical Engineering*, 2014.
- [11] E. Takahashi, R. D. Folkerth, A. M. Galaburda, P. E. Grant, "Emerging Cerebral Connectivity in the Human Fetal Brain: An MR Tractography Study," *Cerebral Cortex* 22 (2), pp. 455-464, 2012.
- [12] T. Zeng, H. Chen, A. Fakhry, X. Hu, T. Liu, S. Ji, "Allen mouse brain atlases reveal different neural connection and gene expression patterns in cerebellum gyri and sulci," *Brain Structure and Function* 220 (5), pp. 2691-2703, 2015.